

Photoluminescent properties of yellow emitting  $\text{Ca}_{1-x}\text{Eu}_x\text{Si}_2\text{O}_{2-\delta}\text{N}_{2+2\delta/3}$  phosphors for white light-emitting diodes

This article has been downloaded from IOPscience. Please scroll down to see the full text article.

2008 J. Phys. D: Appl. Phys. 41 205103

(<http://iopscience.iop.org/0022-3727/41/20/205103>)

View [the table of contents for this issue](#), or go to the [journal homepage](#) for more

Download details:

IP Address: 159.226.165.151

The article was downloaded on 15/10/2012 at 01:39

Please note that [terms and conditions apply](#).

# Photoluminescent properties of yellow emitting $\text{Ca}_{1-x}\text{Eu}_x\text{Si}_2\text{O}_{2-\delta}\text{N}_{2+2\delta/3}$ phosphors for white light-emitting diodes

Meiyuan Wang<sup>1,2</sup>, Jiahua Zhang<sup>1,4</sup>, Xia Zhang<sup>1</sup>, Yongshi Luo<sup>1</sup>, Xinguang Ren<sup>1</sup>, Shaozhe Lu<sup>1</sup>, Xingren Liu<sup>1</sup> and Xiaojun Wang<sup>3</sup>

<sup>1</sup> Key Laboratory of Excited State Processes, Changchun Institute of Optics, Fine Mechanics and Physics, Chinese Academy of Sciences, Changchun 130033, People's Republic of China

<sup>2</sup> Graduate School of Chinese Academy of Sciences, Beijing 100039, People's Republic of China

<sup>3</sup> Department of Physics, Georgia Southern University, Statesboro, GA 30460, USA

E-mail: zhangjh@ciomp.ac.cn

Received 3 June 2008, in final form 15 August 2008

Published 29 September 2008

Online at [stacks.iop.org/JPhysD/41/205103](http://stacks.iop.org/JPhysD/41/205103)

## Abstract

$\text{Ca}_{1-x}\text{Eu}_x\text{Si}_2\text{O}_{2-\delta}\text{N}_{2+2\delta/3}$  phosphors with  $\text{Eu}^{2+}$  concentration ( $x$ ) in the range of 0–0.25 are synthesized by solid-state reaction. With increasing  $x$ , the energy dispersive spectra show that the O/N ratio increases from 0.54 to 1.43 and the emission and excitation spectra show a redshift due to increased splitting of the low-lying  $4f^65d^1$  state of  $\text{Eu}^{2+}$ . An additional excitation band appears at around 460 nm for high doping concentrations of  $\text{Eu}^{2+}$ , perfectly matching the emission wavelength of blue light-emitting diodes (LEDs). The phosphors can be excited in the near-UV to blue region to emit a broad yellow band in the range 543–562 nm, which depends on  $x$ . A white LED is fabricated by combining the  $\text{Ca}_{0.85}\text{Eu}_{0.15}\text{Si}_2\text{O}_{2-\delta}\text{N}_{2+2\delta/3}$  phosphor with a blue GaN chip. Under 20 mA forward-bias current, a CIE chromaticity coordinate of (0.3396, 0.3474), the corresponding colour temperature ( $T_c$ ) of 5223 K, the colour rendering index of 74 and luminous efficiency of  $20 \text{ lm W}^{-1}$  are obtained.

## 1. Introduction

Since the realization of GaN based blue light-emitting diodes (LEDs) [1, 2], white LEDs have been paid much attention for the new generation solid-state lighting. Compared with conventional incandescent and fluorescent lamps, the white LEDs are superior in lifetime, efficiency and reliability, which promises significant reductions in power consumption and in pollution from fossil fuel power plants [3–6]. There are alternative ways to generate white light: the first approach is to mix the light of different colours emitted from different LED chips. Another approach is to mix the emission from a blue or near-UV LED chip with a longer wavelength light down-converted from the LED emission using phosphors [7–11]. Nowadays, the mainstream white LED lamp is a combination of a blue LED semiconductor die and a trivalent cerium activated yttrium-aluminum-garnet (YAG:Ce<sup>3+</sup>) yellow phosphor [12, 13]. Yellow is the

complementary colour of blue, so a mixture of blue light and yellow light exhibits white light [14]. Therefore, the phosphor plays an important role in white-light LED. In the case of white LED phosphors, the inorganic phosphors attract much more attention due to their high luminescent efficiency and long lifetime [15]. But there are very few inorganic yellow phosphors which can combine with a blue chip. The currently commercial yellow phosphor materials for white LED are YAG:Ce<sup>3+</sup> and Sr<sub>3</sub>SiO<sub>5</sub>:Eu<sup>2+</sup>, but YAG:Ce<sup>3+</sup> shows a high thermal quenching [16] and Sr<sub>3</sub>SiO<sub>5</sub>:Eu<sup>2+</sup> shows a poor colour rendition index (CRI = 64) [17]. In recent years, some new yellow emitting oxynitride phosphors such as Ca- $\alpha$ -SiAlON:Eu<sup>2+</sup> and CaSi<sub>2</sub>O<sub>2</sub>N<sub>2</sub>:Eu<sup>2+</sup> have been invented. Though Ca- $\alpha$ -SiAlON:Eu<sup>2+</sup> phosphors have attracted much attention because of their outstanding properties, these kinds of phosphors are prepared at quite high temperature (1800 °C), high pressure (0.925 MPa) and nitridation conditions [18], which are difficult to carry out. In contrast, the CaSi<sub>2</sub>O<sub>2</sub>N<sub>2</sub>:Eu<sup>2+</sup> phosphors only need the usual preparation conditions. Li *et al* reported luminescent properties of

<sup>4</sup> Author to whom any correspondence should be addressed.

$\text{MSi}_2\text{O}_{2-\delta}\text{N}_{2+2\delta/3}:\text{Eu}^{2+}$  ( $M = \text{Ca}, \text{Sr}, \text{Ba}$ ) and suggested that the composition of  $\text{CaSi}_2\text{O}_{2-\delta}\text{N}_{2+2\delta/3}:\text{Eu}^{2+}$  may be somewhat more nitrogen rich than  $\text{CaSi}_2\text{O}_2\text{N}_2:\text{Eu}^{2+}$  ( $\delta = 0$ ), that is,  $\delta > 0$ .

$\text{CaSi}_2\text{O}_{2-\delta}\text{N}_{2+2\delta/3}:\text{Eu}^{2+}$  phosphors can effectively offset the defects of traditional phosphors for white LEDs due to their outstanding properties such as high thermal stability and chemical stability [16]. In particular, they can absorb in the near-UV to blue region and cover a broad section of the colour spectrum, which demonstrate their better luminescent properties and the possibility of improving the CRI of white LED. However, the effect of the  $\text{Eu}^{2+}$  concentration on the luminescence of  $\text{CaSi}_2\text{O}_{2-\delta}\text{N}_{2+2\delta/3}:\text{Eu}^{2+}$  has not been demonstrated.

In this paper, we report the photoluminescence (PL) properties of  $\text{Ca}_{1-x}\text{Eu}_x\text{Si}_2\text{O}_{2-\delta}\text{N}_{2+2\delta/3}$  as a function of  $\text{Eu}^{2+}$  concentrations. The  $\text{Ca}_{1-x}\text{Eu}_x\text{Si}_2\text{O}_{2-\delta}\text{N}_{2+2\delta/3}$  phosphors include both nitrogen rich, i.e.  $\delta > 0$  and oxygen rich, i.e.  $\delta < 0$  compositions. White LED is fabricated by combining 460 nm emitting GaN chip with  $\text{Ca}_{1-x}\text{Eu}_x\text{Si}_2\text{O}_{2-\delta}\text{N}_{2+2\delta/3}$  phosphor for  $x = 0.15$ .

## 2. Experimental

A series of samples, the undoped and  $\text{Eu}^{2+}$ -doped  $\text{Ca}_{1-x}\text{Eu}_x\text{Si}_2\text{O}_{2-\delta}\text{N}_{2+2\delta/3}$  ( $x = 0-0.25$ ) phosphors are prepared by a high-temperature solid-state reaction technique. The starting materials are CaO (analytical grade),  $\text{SiO}_2$  (analytical grade),  $\text{Si}_3\text{N}_4$  (analytical grade) and  $\text{Eu}_2\text{O}_3$  (99.99%). The raw materials are taken in an agate mortar in stoichiometric molar ratio and ground for 1 h, and then the mixture is loaded into alumina crucibles and sintered at 1380 °C for 4 h in a horizontal tube furnace under a weak reductive atmosphere (5% $\text{H}_2$  + 95% $\text{N}_2$  mixed flowing gas), followed by additional grinding. The crystal structures of all the samples are checked using conventional x-ray diffraction (XRD). PL excitation (PLE) and PL spectra are measured using a fluorescent spectrophotometer (F-4500, Hitachi Ltd, Japan) equipped with a Xe lamp as an excitation source; at the same time the diffuse reflection spectra are obtained by a  $\text{BaSO}_4$  white powder as the standard reference. The decay curves are recorded by a TDS3052 (digital phosphor) oscilloscope. The white LED is fabricated by a combination of a blue GaN chip and the prepared  $\text{Ca}_{1-x}\text{Eu}_x\text{Si}_2\text{O}_{2-\delta}\text{N}_{2+2\delta/3}$  ( $x = 0.15$ ) phosphor. The LED spectrum is measured using a USB4000 spectrophotometer.

## 3. Results and discussion

### 3.1. XRD analysis

Figure 1 shows the powder diffraction patterns of the undoped and  $\text{Eu}^{2+}$ -doped  $\text{CaSi}_2\text{O}_{2-\delta}\text{N}_{2+2\delta/3}$  synthesized at 1380 °C in a weak reductive atmosphere. The XRD patterns are collected in the range  $18^\circ \leq 2\theta \leq 60^\circ$ . The powder diffraction patterns of  $\text{Ca}_{1-x}\text{Eu}_x\text{Si}_2\text{O}_{2-\delta}\text{N}_{2+2\delta/3}$  are essentially close to those reported for  $\text{CaSi}_2\text{O}_{2-\delta}\text{N}_{2+2\delta/3}$  ( $\delta \geq 0$ ) by Y Q Li and H T Hintzen. They have a monoclinic crystal structure [16]

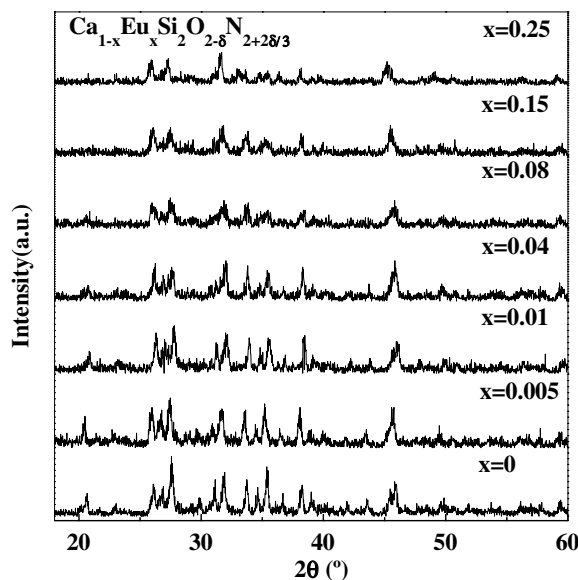


Figure 1. XRD patterns of  $\text{Ca}_{1-x}\text{Eu}_x\text{Si}_2\text{O}_{2-\delta}\text{N}_{2+2\delta/3}$  ( $x = 0-0.25$ ).

and the particle size is about 1  $\mu\text{m}$ . For low and high  $\text{Eu}^{2+}$  concentrations, the strongest XRD peak is at about  $27.58^\circ$  and  $31.91^\circ$ , respectively. Energy dispersive spectra (EDS) of  $\text{Ca}_{1-x}\text{Eu}_x\text{Si}_2\text{O}_{2-\delta}\text{N}_{2+2\delta/3}$  are measured. The O/N ratios are listed in table 1. It is clearly observed that the O/N ratio increases from 0.54 to 1.43 with an increase in the  $\text{Eu}^{2+}$  concentration from 0 to 0.25. Therefore, the position changes of the strongest XRD peak may be due to the effect of the increased O/N ratios. A similar effect was also observed in  $\text{SrSi}_2\text{O}_{2-\delta}\text{N}_{2+2\delta/3}$  as the O/N ratio was increased [16].

### 3.2. The diffuse reflectance spectra

Figure 2 shows the diffuse reflectance spectra of  $\text{CaSi}_2\text{O}_{2-\delta}\text{N}_{2+2\delta/3}$  and  $\text{Eu}^{2+}$ -doped  $\text{CaSi}_2\text{O}_{2-\delta}\text{N}_{2+2\delta/3}$ . The daylight colour of the undoped  $\text{CaSi}_2\text{O}_{2-\delta}\text{N}_{2+2\delta/3}$  compound is grey-white, and its diffuse reflectance spectrum is almost a flowing line, which illustrates that the  $\text{CaSi}_2\text{O}_{2-\delta}\text{N}_{2+2\delta/3}$  compound does not have absorption. As for the doped samples, strong absorption bands are presented in the range of the UV to visible spectral region, which can be assigned to the  $4f^7 \rightarrow 4f^65d^1$  transition of the  $\text{Eu}^{2+}$  ion. It is obvious that with an increase in  $\text{Eu}^{2+}$  concentration (0.005–0.25), the absorption of  $\text{Eu}^{2+}$  becomes markedly stronger and the absorption band edge shifts to the longer wavelength side so that the body colour of the phosphors reddens gradually.

### 3.3. PLE and PL spectra

Figure 3 shows the PLE and PL spectra of  $\text{Ca}_{1-x}\text{Eu}_x\text{Si}_2\text{O}_{2-\delta}\text{N}_{2+2\delta/3}$  ( $x = 0.005-0.25$ ) phosphors with different  $\text{Eu}^{2+}$  concentrations. The PLE spectrum lies in the UV to blue spectral region, which is attributed to the  $4f^7 \rightarrow 4f^65d^1$  transition of  $\text{Eu}^{2+}$ . With increasing  $\text{Eu}^{2+}$  concentrations, the PLE band edge shifts to the longer wavelength side, following the formation of a strong excitation band at around 460 nm, which matches the blue LED chip very well. This band

**Table 1.** The mole ratios of O to N in  $\text{Ca}_{1-x}\text{Eu}_x\text{Si}_2\text{O}_{2-\delta}\text{N}_{2+2\delta/3}$  ( $x = 0-0.25$ )

At %	$x = 0$	$x = 0.005$	$x = 0.01$	$x = 0.04$	$x = 0.08$	$x = 0.15$	$x = 0.25$
O/N	0.54	0.69	1.03	1.25	1.03	1.26	1.43

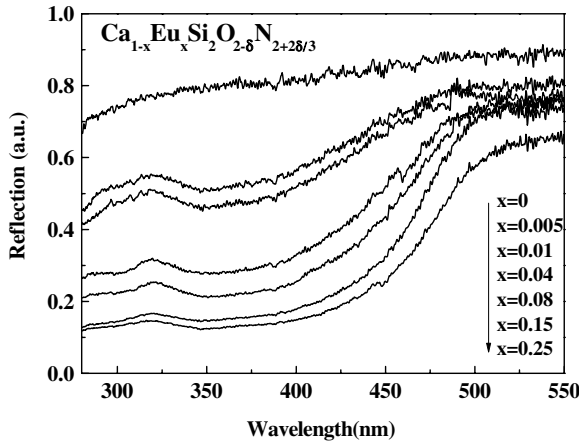


**Figure 2.** Diffuse reflectance spectra of  $\text{CaSi}_2\text{O}_{2-\delta}\text{N}_{2+2\delta/3}$  and  $\text{Ca}_{1-x}\text{Eu}_x\text{Si}_2\text{O}_{2-\delta}\text{N}_{2+2\delta/3}$  ( $x = 0.005-0.25$ ).

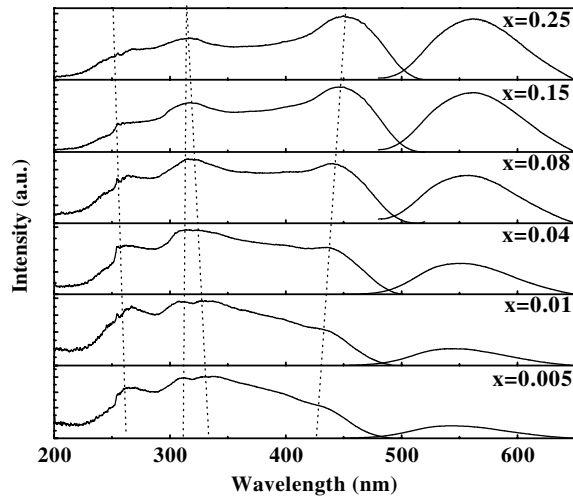


**Figure 3.** The excitation and emission spectra ( $\lambda_{\text{exc}} = 460 \text{ nm}$ ) of  $\text{Ca}_{1-x}\text{Eu}_x\text{Si}_2\text{O}_{2-\delta}\text{N}_{2+2\delta/3}$  ( $x = 0.005-0.25$ ).

becomes stronger with an increase in  $\text{Eu}^{2+}$  concentrations. A similar result has been reported in  $\text{Sr}_{2-y}\text{Eu}_y\text{Al}_{1.6}\text{Si}_{1.4}\text{O}_{6.6}\text{N}_{0.4}$  by Li [19].

The PL spectrum for 460 nm excitation shows a single broad yellow band, which also shifts to the longer wavelength side from 543 to 562 nm with increasing  $\text{Eu}^{2+}$  concentrations from 0.005 to 0.25, and the full-width half-maximum (FWHM) is about 63 nm. The emission band is ascribed to the  $4f^65d^1 \rightarrow 4f^7$  transition of divalent europium [18], and the broadness of the emission band indicates a strong interaction between the host and the activators [20]. In the PLE spectrum, there are three other PLE peaks located at about 266 nm, 310 nm and 331 nm, respectively. The 266 nm and 331 nm peaks shift to the blue side and the 310 nm peak shifts to the red side with increasing  $\text{Eu}^{2+}$  concentrations, and both the 310 nm and the 331 nm peaks shift to 315 nm for high  $\text{Eu}^{2+}$  concentrations.

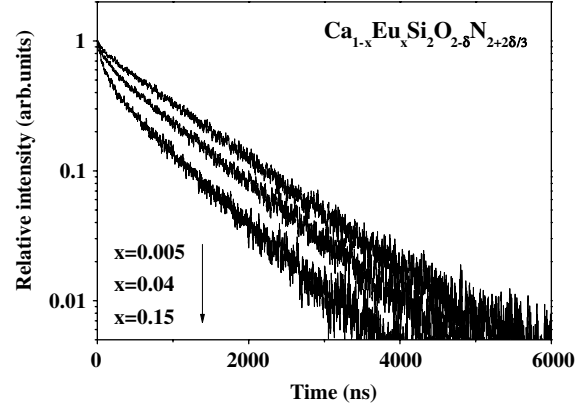


**Figure 4.** Fluorescence lifetimes of  $\text{Ca}_{1-x}\text{Eu}_x\text{Si}_2\text{O}_{2-\delta}\text{N}_{2+2\delta/3}$  ( $x = 0.005, 0.04, \text{ and } 0.15$ ).

The redshift of the PLE band edge exhibits an increase in the energy separation between the band edge and the three other peaks, clearly demonstrating an enhanced splitting of the low-lying  $4f^65d^1$  state of  $\text{Eu}^{2+}$ , as shown in figure 3. The increased splitting implies the enhanced crystal field strength due to the modified local structure of  $\text{Eu}-(\text{O}, \text{N})$  by increasing the O/N ratio at high  $\text{Eu}^{2+}$  concentrations. The increased splitting then leads to a redshift of emission and excitation spectra as well as the formation of the 460 nm PLE band [19].

### 3.4. Fluorescence lifetimes

Figure 4 shows the fluorescence decay curves with normalized initial intensities in  $\text{Ca}_{1-x}\text{Eu}_x\text{Si}_2\text{O}_{2-\delta}\text{N}_{2+2\delta/3}$  ( $x = 0.005, 0.04 \text{ and } 0.15$ ) monitored at 530 nm. By integrating the area under the decay curves, the fluorescence lifetimes are obtained. The lifetimes decrease with an increase in the dopant ions in the host matrix, and the decay curves show a single exponential behaviour for low  $\text{Eu}^{2+}$  concentrations ( $x < 0.04$ ), but nonexponential behaviour for high  $\text{Eu}^{2+}$  concentrations ( $x = 0.15$ ). The phenomena are the well-known effect of energy transfer among  $\text{Eu}^{2+}$  ions, in which transfer rates are not constant but have a distribution [21].

### 3.5. Dependence of PL intensities on $\text{Eu}^{2+}$ concentrations

Figure 5(a) shows the dependence of luminescent intensities under 460 nm excitation and fluorescent lifetimes on  $\text{Eu}^{2+}$  concentrations. The luminescent intensities reach the maximum at  $x = 0.08$  and tend to be saturated as  $x$  is higher than 0.08. The luminescent lifetime monotonically decreases with increasing  $\text{Eu}^{2+}$  concentrations. The lifetimes can reflect the emission efficiencies because they are obtained by integrating the area under the decay curves. The luminescent intensities ( $I$ ) are, therefore, proportional to luminescent lifetimes ( $\tau$ ) and obviously also to the absorbed photon

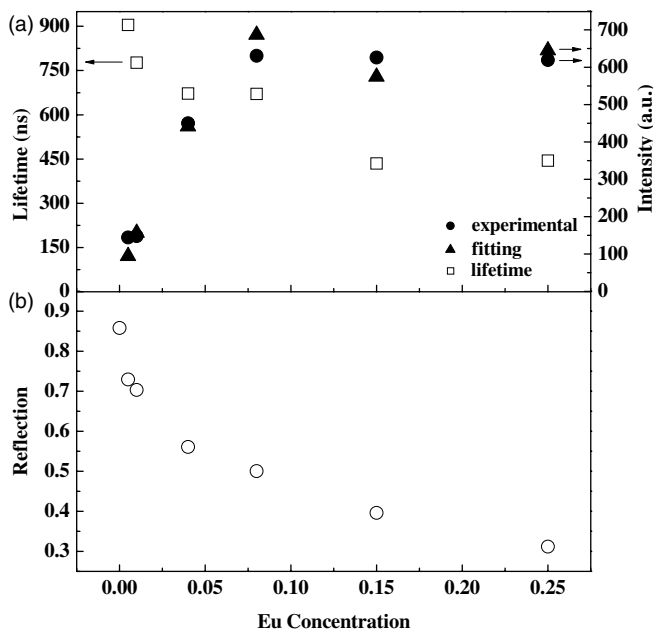


**Figure 5.** Luminescence intensity, lifetime (a) and diffuse reflectance (b) of  $\text{Ca}_{1-x}\text{Eu}_x\text{Si}_2\text{O}_{2-\delta}\text{N}_{2+2\delta/3}$  ( $x = 0.005\text{--}0.25$ ) measured at room temperature as a function of  $\text{Eu}^{2+}$  concentration.

numbers ( $n$ ) of excitation light.  $n$  is proportional to the term of  $1 - \exp(-x/x_c)$ , where  $x_c$  is a critical  $\text{Eu}^{2+}$  concentration for absorption saturation. Then, luminescent intensity can be written as  $I = A[1 - \exp(-x/x_c)]\tau$  with a constant  $A$ . Using this equation and the measured lifetimes to fit the measured luminescent intensities for various  $x$ , the value of  $x_c$  is obtained to be about 0.07. The good fitting results are presented in figure 5(a).

Figure 5(b) shows the diffuse reflectance at 460 nm as a function of  $\text{Eu}^{2+}$  concentrations. The reflectance tends to saturation as  $x$  is higher than 0.08, indeed indicating the performance of absorption saturation for  $x$  higher than  $x_c$ , as estimated above.

### 3.6. A white LED using a blue GaN chip and $\text{Ca}_{1-x}\text{Eu}_x\text{Si}_2\text{O}_{2-\delta}\text{N}_{2+2\delta/3}$ ( $x = 0.15$ ) phosphor

In order to investigate the luminescent properties of the phosphor in white LED, a white LED is fabricated by combination of a blue GaN chip and the prepared  $\text{Ca}_{1-x}\text{Eu}_x\text{Si}_2\text{O}_{2-\delta}\text{N}_{2+2\delta/3}$  ( $x = 0.15$ ) phosphor. Figure 6 shows the electroluminescent spectrum of the as-fabricated white LED at forward-bias current  $I_F = 20$  mA. Two distinct emission bands in blue and yellow are clearly observed in the emission spectrum of the PC-LED. They are from the blue LED chip and the phosphor, respectively. The generated white light shows CIE chromaticity coordinates of (0.3396, 0.3474), the correlated colour temperature ( $T_c$ ) of 5223 K, the colour rendering index (CRI) of 74 and luminous efficacies of  $20 \text{ lm W}^{-1}$ .

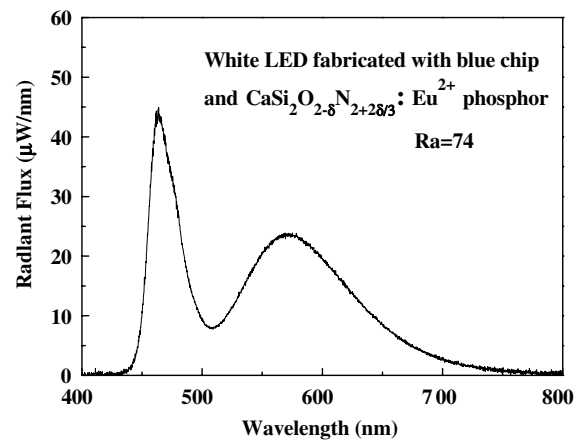


**Figure 6.** The electroluminescence spectra of the fabricated pc-LED combined with  $\text{Ca}_{1-x}\text{Eu}_x\text{Si}_2\text{O}_{2-\delta}\text{N}_{2+2\delta/3}$  ( $x = 0.005\text{--}0.25$ ) phosphor under 20 mA forward-bias current.

## 4. Conclusions

In summary, we have synthesized a yellow emitting  $\text{Ca}_{1-x}\text{Eu}_x\text{Si}_2\text{O}_{2-\delta}\text{N}_{2+2\delta/3}$  ( $x = 0.005\text{--}0.25$ ) phosphor by high-temperature solid-state reaction for creating daylight emission from PC-LED. The phosphor emits a yellow broadband in the range 543–562 nm, with FWHM of about 63 nm. The PL intensity of  $\text{Ca}_{1-x}\text{Eu}_x\text{Si}_2\text{O}_{2-\delta}\text{N}_{2+2\delta/3}$  is found to be saturated for  $x \geq 0.08$ . This is attributed to the saturation of absorption of excitation light, which is supported by the diffuse reflectance spectra and  $\text{Eu}^{2+}$  concentrations dependent PL intensities. With an increase in  $\text{Eu}^{2+}$  concentrations, the O/N ratio increases, and the splitting of the low-lying  $4f^65d$  states of  $\text{Eu}^{2+}$  is enhanced, with the result that the tail of the excitation spectrum shifts to the longer wavelength, and an additional excitation band appears at around 460 nm, perfectly matching the emission wavelength of blue LEDs. A white light-emitting LED is fabricated by a combination of a blue GaN chip and the prepared  $\text{Ca}_{0.85}\text{Eu}_{0.15}\text{Si}_2\text{O}_{2-\delta}\text{N}_{2+2\delta/3}$ . The white LED exhibits CIE chromaticity coordinates of (0.3396, 0.3474), the correlated colour temperature ( $T_c$ ) of 5223 K, the CRI of 74 and luminous efficacies of  $20 \text{ lm W}^{-1}$ . The outstanding luminescent properties and high thermal stability indicate that further development of the  $\text{CaSi}_2\text{O}_{2-\delta}\text{N}_{2+2\delta/3} : \text{Eu}^{2+}$  phosphor could be an attractive topic for white LEDs.

## References

- [1] Nakamura S, Senoh M and Mukai T 1993 *Appl. Phys. Lett.* **62** 2390
- [2] Yan S X, Zhang J H, Zhang X, Lu S Z, Ren X G, Nie Z G and Wang X J 2007 *J. Phys. Chem. C* **111** 13256
- [3] Li Y Q, Steen J E J van, Kreveld J W H van, Botton G, Delsing A C A, DiSalvo F J, De With G and Hintzen H T 2006 *J. Alloys Compounds* **417** 273
- [4] Wang Z L, Liang H B, Wang J, Gong M L and Su Q 2006 *Appl. Phys. Lett.* **89** 071921
- [5] Zhang N, Wang D J, Li L, Meng Y S, Zhang X S and Ming N 2006 *J. Rare Earths* **24** 294
- [6] Piao X Q, Machida K I, Horikawa T, Hanzawa H, Shimomura Y and Kijima N 2007 *Chem. Mater.* **19** 4592

- [7] Nakamura S 1997 *Proc. SPIE* **26** 3002
- [8] Shur M S and Zukauskas A 2005 *Proc. IEEE* **93** 1691
- [9] Park J K, Lim M A, Kim C H, Park H D, Park J T and Choi S Y 2003 *Appl. Phys. Lett.* **82** 683
- [10] Kim J S, Jeon P E, Choi J C, Park H L, Mho S I and Kim G C 2004 *Appl. Phys. Lett.* **84** 2931
- [11] Hao Z D, Zhang J H, Zhang X, Sun X Y, Luo Y S and Lu S Z 2007 *Appl. Phys. Lett.* **90** 261113
- [12] Sakuma K, Hirosaki N and Xie R J 2007 *J. Lumin.* **126** 843
- [13] Guo C F, Huang D and Su Q 2006 *Mater. Sci. Eng. B* **130** 189
- [14] Zhao X X, Wang X J, Chen B J, Meng Q Y, Di W H, Ren G Z and Yang Y M 2007 *J. Alloys Compounds* **433** 352
- [15] Xie R J, Hirosaki N and Mitomo M 2006 *Appl. Phys. Lett.* **88** 101104
- [16] Li Y Q, Delsing A C, With G D and Hintzen H T 2005 *Chem. Mater.* **17** 3242
- [17] Park J K, Kim C H, Park S H and Park H D 2004 *Appl. Phys. Lett.* **84** 1647
- [18] Xie R J and Hirosaki N 2004 *Appl. Phys. Lett.* **84** 5404
- [19] Li Y Q, Hirosaki N, Xie R J and Mitomo M 2007 *Sci. Technol. Adv. Mater.* **8** 607
- [20] Park J Ku, Lim M A, Kim C H and Park H D 2003 *Appl. Phys. Lett.* **82** 5
- [21] Park W, Jones T C, Tong W, Schön S, Chaichimansour M, Wagner B K and Summers C J 1998 *J. Appl. Phys.* **84** 6852